HEFAT2007
5th International Conference on Heat Transfer, Fluid Mechanics and Thermodynamics
Sun City, South Africa
Paper number: OR1

AN EXPERIMENTAL AND COMPUTATIONAL STRATEGY FOR AN INCREASED UNDERSTANDING OF TWO-PHASE FLOW OF NATURAL GAS

Olsen R.*[−], Maråk K.A.[+], Zhao H.[+] and Munkejord S.T.[−]
*Author for correspondence
[−]Department of Energy Processes,
SINTEF Energy Research,
Trondheim, Norway,
E-mail: robert.olsen@sintef.no
[+]Department of Energy and Process Engineering,
Norwegian University of Science and Technology (NTNU)

ABSTRACT

This paper presents a research strategy aimed towards understanding transient two-phase flow in compact low-temperature equipment, with emphasis on heat exchangers. The strategy is based on the hypotesis that to meet the many two-phase challenges occurring in compact process equipment, detailed knowledge about basic flow phenomena is needed. To provide this knowledge, a relevant computer simulation model and experimental setups are under development. The computer model is based on the level-set method, which is suitable for detailed two-phase flow calculations, and which has been shown to be able to reproduce flow phenomena observed in small channels. Two experimental setups are presented, one for measuring details regarding flow topology, such as film behaviour, droplet tear-off, droplet-droplet and droplet-film interaction, and a second for measuring integral quantities like pressure drop and heat transfer during condensation of natural gas mixtures in microtubes. The tubes range from 0.25–1 mm in diameter and the experiments will be performed at low temperatures. This setup will provide data to design compact heat exchangers.

INTRODUCTION

Production of *Liquefied Natural Gas* (LNG) on offshore installations has been a focused area for several oil companies over the last decade. The main challenges in realizing offshore floating LNG production plants is the reduction of weight and volume, and keeping the process equipment robust to acceleration and tilting, [1]. To overcome these challenges, new compact equipment must be designed and analysed. Although computational fluid dynamics (CFD) models have been developed over the last decades and may act as support in the design phase, it is still necessary to verify and develop them further to fulfill this task.

For a compact heat exchangers to operate at maximum performance and to minimize exergy losses, one must ensure that the working fluid is correctly distributed while minimizing the pressure losses. One way to achieve compact heat exchangers is to reduce the hydraulic diameter, [2]. To distribute a two-phase flow from one channel to as many as one million small channels evenly, a thorough understanding of basic flow phenomena is needed. Further, all of the working fluid must have evaporated before entering the compressor. If droplets are torn off the liquid surface due to gas drag and film instability, the heat exchanger needs to be extended unnecessarily to enforce full evaporation. Another challenge is the large temperature gradients which may occur due to sudden changes in operation, which again induce stresses on the construction.

A thorough understanding of the processes and phenomena occurring at a small-scale level in the heat exchanger is necessary to obtain an improved understanding of the whole heat exchanger and its design.

Some elements of current heat exchanger design are:

- The use of engineering correlations of limited accuracy and generality.
- Full-scale testing.
- Oversizing to compensate for unexpected effects.

Oversizing and full-scale testing are both expensive, and full-scale testing is time consuming. Moreover, oversizing may be unacceptable for new floating facilities, where space and weight considerations are important, and where a posteriori design modifications may be difficult or impossible.

If the initial heat exchanger design could be made more accurate, then both full-scale testing and oversizing could be reduced. This is the ambitious long-term goal pursued here, by employing a dual research methodology:

- Developing and employing detailed mathematical/numerical models describing the relevant phenomena.
- Conducting detailed and careful laboratory experiments to study the same phenomena.

The path of developing a well-tested and detailed mathematical/numerical model is long and winding, but once it is completed, numerical «experiments» can be carried out much faster and cheaper, and over a broader range of parameters than in the laboratory. Moreover, the development of the mathematical model may in itself help the researchers to better understand the observed phenomena. It almost goes without saying that high-quality experimental data are required for the model development. This is both to validate (or invalidate) the numerical results produced, but also to give an insight into «reality», which is necessary for choosing an applicable modelling approach.

Basic phenomena to investigate

Liquid film - Roques and Thome [3] found three flow patterns on a vertical array of horizontal tubes. In the examination of a flowing liquid film, the flow pattern and wavyness needs to be described.

Deformation - A droplet will basically maintain its shape before interaction, while during and after the interaction, its shape will deform and oscillate. A description of how a droplet deforms during its interactions, includes a dimensionless number, D_w/D_h (The width-height ratio during the deformation) [4]. The dimensionless number, t/t_i, (where t is the real time and $t_i = D/U_i$ is the impact time-scale, D the diameter, and U_i the impact velocity) expresses the width-height ratio versus time.

Coalescence and coalescence threshold - The phenomenon of coalescence happens when a droplet interacts with another droplet or a liquid film. Research has been done [5] with focus on coalescence and bouncing transition of aerosol droplets, and the Weber number, the Ohnesorge number and the Knudsen number were used for correlating the transition phenomena. The Weber number can be seen as dimensionless velocity which denotes the impact energy. It is reasonable to assume that at low Weber numbers, the impact energy of droplets will be converted to deformation and oscillation energy at the interfaces, and finally the deformation energy will lead to bouncing of droplets in the opposite direction. Increasing the Weber number will lead to break up of the interface film in the end. The coalescence threshold is thus interpreted by a critical Weber number at which the interface film breaks up.

Spreading - This phenomenon exists only when a droplet impacts on a dry surface. Spreading is usually described by different relations between contact angle and other dimensionless numbers [6].

Splashing and splashing threshold - The phenomenon of splashing can happen when a droplet impacts on either a dry surface or a liquid surface. A splashing threshold exists when spreading or coalescence reaches a critical point. Wang and Chen [7] used the Weber number as the parameter to judge the threshold of a glycerol-water droplet splashing on the same liquid film. The Weber number is the most important in threshold judgment, but it is not the only parameter that should be considered [6]. It is found by Stow and Hadfield [8] that the splashing threshold of a water droplet on an unyielding dry surface can be decided by a relation between the surface roughness and an expression combining the Reynolds number

and the Weber number.

MODELLING OF TWO-PHASE FLOW IN HEAT EXCHANGERS

We believe that further developing the knowledge of two-phase flow behavior on a micro-scale level will improve the physical understanding and modelling of two-phase flow phenomena also on a medium scale. An improved physical understanding may contribute to design innovations. An improved modelling can further develop the design and reveal operational issues at an early stage.

Microscale flow

There is no generally accepted criterion for microscale flow, but the definition in Equation (1) from [9] can be used as a guideline.

$$d \leq \sqrt{\frac{4\sigma}{g(\rho_{\mathrm{L}} - \rho_{\mathrm{G}})}}, \tag{1}$$

where d is the hydraulic diameter. Research on microscale two-phase flow is still in its infancy. As demonstrated by Thome [10], several difficulties have yet to be overcome to predict microscale two-phase flow in a satisfactory manner. The biggest problem is that the models developed for macroscale are not necessarily valid for microscale flow, and no good replacements exist. In addition, experimental studies on microscale natural gas are hard to find.

When it comes to the modelling of two-phase flow, we also think of scales in an another aspect. Large-scale models have assumptions on the physics occuring on a smaller scale. Different models with different assumptions of sub-scale modelling are shown in Figure 1.

To model the pressure drop and heat transfer in the channels, mainly stationary correlations are used, and examples of such large scale correlations are given by e.g. Lockhart-Martinelli [11], Chisholm [12], Friedel [13], Model for annular flow Chisholm [14], p.122-124, and Müller-Steinhagen [15].

These correlations are developed within a specific range of the different parameters and must be used with care for new fluids or different geometries.

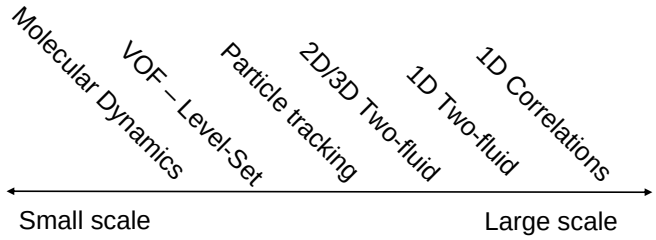

Figure 1: Models and scale in the sense of assumptions of subscale physics.

If dynamic behavior needs to be calculated, the one dimensional two-fluid model is frequently used. The two-fluid model relies on assumptions of flow regime and subscale models for interfacial mass and momentum transfer. For instance there is no information in the two-fluid model about whether the flow is mist or separated, since the interface is not explicitly calculated. There have been attempts to extend the two-fluid model to two and three dimensions to calculate larger scale interfaces, however there are many challenges left [16].

More detailed models, such as the level-set method and the VOF method, which track the interface, have been proposed. The VOF method reconstructs the interface, while the level-set method introduces the level-set function as the distance to the interface. Then an equation for the advection of the level-set function is solved.

The calculation of basic phenomena occuring in flow of two-phase hydrocarbon mixtures is still in the start phase. A first examination of the applicability of the level-set method to flow of natural gas has been performed, and the capability to predict a transition from annular to bubbly flow has been demonstrated in a two-dimensional calculation, see Figure 2. The details can be found in Teigen [17]. A basic presentation of the theory of the level-set method is given in the next section.

THE LEVEL-SET METHOD

The volume of fluid and level-set methods solve the governing equations on a fixed grid. They are often referred to as front-capturing methods. In the vof method, the interface is reconstructed based on the calculated mass fraction. The level-set method employs a scalar function advected with the interface velocity. From this function, the interface and its geometric properties are calculated. In this section we present the basis for the level-set method.

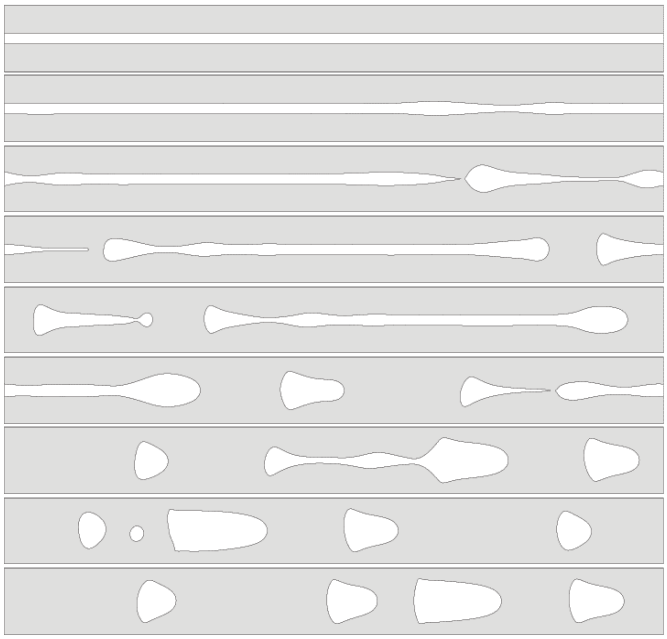

Figure 2: Selection of frames from $T = -120\,^{\circ}\mathrm{C}$, showing a transition from annular to bubble flow. From top to bottom, $t = [0; 4.8; 11.1; 12.3; 13.2; 15.6; 18.9; 23.4; 40.2]$ ms.

Implicit surfaces

An implicit surface is defined as the isocontour of a given function. Let $\phi(\vec{x})$ be the function, and let the zero isocontour, or $\partial\Omega$, represent the interface. Define the gas phase as $\phi < 0$, or Ω^-, and the liquid phase as $\phi > 0$ or Ω^+. For the surface, the unit normal is

$$\vec{n} = \frac{\nabla\phi}{|\nabla\phi|}, \tag{2}$$

and the curvature

$$\kappa = \nabla \cdot \vec{n} = \nabla \cdot \left(\frac{\nabla\phi}{|\nabla\phi|}\right). \tag{3}$$

Distance functions

A distance function for the interface, $d(\vec{x})$, is defined as

$$d(\vec{x}) = \min(|\vec{x} - \vec{x}_I|) \text{ for all } \vec{x}_I \in \partial\Omega, \tag{4}$$

where x_I represents the points on the interface. Define ϕ so that $|\phi(\vec{x})| = d(\vec{x})$. Thus, $\phi = 0$ for all $\vec{x} \in \partial\Omega$, $\phi = -d(\vec{x})$ for all $\vec{x} \in \Omega^-$ and $\phi = d(\vec{x})$ for all $\vec{x} \in \Omega^+$. From this follows that

$$|\nabla\phi| = 1, \tag{5}$$

the unit normal, Equation (2), simplifies to

$$\vec{n} = \nabla\phi, \tag{6}$$

and the curvature, Equation (3), to

$$\kappa = \nabla^2\phi. \tag{7}$$

Level-set method

The level-set method adds dynamics to implicit surfaces. In order to evolve the interface, the following convection equation is solved in addition to the equations of motion:

$$\frac{\partial\phi}{\partial t} + \vec{u} \cdot \nabla\phi = 0. \tag{8}$$

Reinitialization of the level-set function

Because of numerical errors, ϕ will not remain an exact distance function. ϕ is therefore reinitialized to a distance function for every time step. As shown in [18], this can be accomplished by solving the following equation to steady state:

$$\frac{\partial\phi}{\partial t} + S(\phi_0)(|\nabla\phi| - 1) = 0, \tag{9}$$

where S is a numerically smeared out sign function:

$$S(\phi_0) = \frac{\phi_0}{\sqrt{\phi_0^2 + (\Delta x)^2}}, \tag{10}$$

and ϕ_0 is the initial level-set function at the current timestep.

Equations of motion

The two phases are governed by the Navier-Stokes equations for incompressible flow:

$$\nabla \cdot \vec{u} = 0 \tag{11}$$

$$\frac{\partial \vec{u}}{\partial t} + \vec{u} \cdot \nabla \vec{u} = -\frac{\nabla p}{\rho} + \frac{\nabla \cdot \tau}{\rho} - \frac{\sigma \kappa \delta \vec{n}}{\rho} + \vec{F}, \quad (12)$$

where τ is the viscous stress tensor and $\vec{F}$ is a body force, e.g. gravity. The second to last term is an interface term and described in [18]. σ is the coefficient of surface tension, κ is the curvature of the interface, δ is the Dirac delta function and $\vec{n}$ the unit normal vector.

Density and viscosity are discontinuous across the interface. To avoid problems with this discontinuity, a smeared-out definition of these quantities is used:

$$\rho(\phi) = \rho^- + (\rho^+ - \rho^-)H(\phi), \quad (13)$$

and

$$\mu(\phi) = \mu^- + (\mu^+ - \mu^-)H(\phi), \quad (14)$$

where H is a numerically smeared-out Heaviside function,

$$H(\phi) = \begin{cases} 0 & \phi < -\epsilon \\ \frac{1}{2} + \frac{\phi}{2\epsilon} + \frac{1}{2\pi}\sin(\frac{\pi\phi}{\epsilon}) & -\epsilon \leq \phi \leq \epsilon \\ 1 & \phi > \epsilon \end{cases} \quad (15)$$

An ϵ of $1.5\Delta x$ is used, i.e. the quantities are smeared out over three grid cells. The area of the two phases can now be calculated as

$$A^+ = \int_\Omega H(\phi(\vec{x}))\mathrm{d}A, \quad (16)$$

$$A^- = \int_\Omega 1 - H(\phi(\vec{x}))\mathrm{d}A. \quad (17)$$

A full three dimensional calculation is needed to accurately predict the phenomena in Figure 2 and most other occuring in two-phase flow. There is a also a need to verify the calculation method and understand how it should be further developed. To do this, experimental studies of hydrocarbon mixtures are needed, see the section on experiments on micro-scale flow phenomena.

Even if all the basic phenomena can be correctly described by computations, measurements of integral quantities like heat transfer and pressure drop are still needed. Below, we present an experimental setup designed to provide data for correlations during condensation of natural gas. Besides providing data for pressure drop and heat transfer, within this apparatus, visualisation of the flow can be made possible.

The aim of the development of the level-set method is to calculate the flow behavior of these experiments. If this is shown to be possible, the level-set method has good prospects to act as a supplement to complex experiments and provide knowledge about two-phase flow.

EXPERIMENTAL SETUP FOR MEASURING HEAT TRANSFER IN MICROCHANNELS DURING CONDENSATION OF NATURAL GAS

The purpose of the described rig is to gain an understanding of heat transfer in condensing multi-component mixtures in microchannels. The results can be used to design an industrial scale heat exchanger based on microchannels.

A similar rig was built by Grohmann [19]. He measured flow boiling of argon at temperatures around 120 K in tubes with diameters of 250 μm and 500 μm. The purpose of his work was to investigate the potential of miniaturised cooling for low-temperature applications such as tracking detectors in particle accelerators.

As will be shown later, parts of the experimental setup is calibrated using a correlation for single phase heat transfer in turbulent flow in smooth pipes, and the correlation by Gnielinski [20] is used. For $2300 < Re < 10^6$:

$$Nu = a\left(Re^{0.87} - b\right) Pr^{0.4}\left[1 + \left(\frac{d}{L}\right)^{2/3}\right]\left(\frac{\mu}{\mu_w}\right)^{0.25} \quad (18)$$

where for liquids $a = 0.012$ and $b = 280$. Nu the nusselt number, Re the Reynolds number, Pr the Prandtl number, d the tube diameter, L the tube length and μ the kinematic viscosity. As the velocity profile for turbulent flow is fully developed, the thermal entry length effects can be adjusted for by the term $1 + \left(\frac{d}{L}\right)^{2/3}$ [20]. The term $\left(\frac{\mu}{\mu_w}\right)^{0.25}$ corrects for varying fluid properties due to the temperature gradients in the flow, in this case because of cooling (Kays *et al.* [21] quoting Petukhov [22]).

Experimental setup

The test rig and measurement concept was designed by Grohmann [23].

The experimental setup is designed to measure both single and two phase heat transfer (cooling and condensing)

and pressure drop in small channels with $d \geq 2$ mm. Its temperature range is approx. 45-300 K and the maximum pressure is 70 bar, which means that a number of fluids and fluid mixtures can be used. The maximum flow rate is $\dot{m} = 2.5 \cdot 10^{-3}$ kg/s.

With modifications of the setup, it is also possible to measure flow boiling heat transfer.

In Figure 3 a schematic overview of the experimental rig. The experimental rig consists of a warm and a cold part, where the cold part, holding the test section, is contained inside a vacuum chamber. The working fluid is circulated through both and undergoes a number of phase changes. The cooling is provided by a Stirling cryocooler. The compressor between point 1 and 2, in Figure 3, supplies the circulation in the system. The water cooler between point 2 and 3 cools the gas from the compressor. A needle valve is used to adjust the ratio of bypass flow back to the compressor. From point 3, the gas goes through an oil separator, followed by an oil and particle filter and a flow meter. Inside the vacuum chamber, the gas is first cooled in the internal heat exchanger (point 4), after which it is condensed and sub-cooled in the hollow thermal interface (point 5).

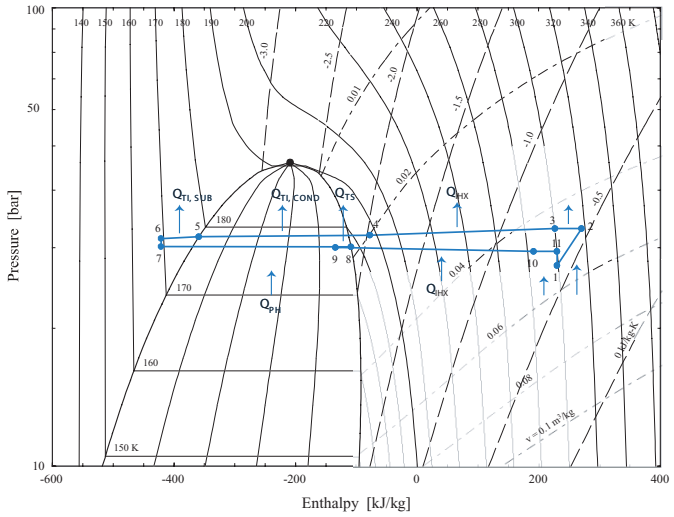

Figure 4: Pressure-enthalpy diagram of the test rig cycle, in this case for heat transfer of condensing methane at high vapour quality.

From point 7 to 8, the fluid enters the pre-heater, which for two phase measurements controls the vapour quality of the fluid before it enters the test section. From point 9, where the heat transfer and pressure drop measurement take place, the fluid passes through the internal heat exchanger again in order to cool down the incoming fluid. Between point 11 and 1, a suction pressure regulator also helps control the flow rate.

In Figure 4, the distance from point 8 to 9 shows the enthalpy change in the test section, and this distance is adjusted by another heater $\dot{Q}_{HS}$. $\dot{Q}_{IHX}$ denotes the heat transferred in the internal heat exchanger, while the heat fed between 10 to 11 is heat leakage from the surroundings.

The test tube in Figure 5 is a stainless steel tube soldered to a copper block, which again is connected to a copper rod. This rod works as a measurement device for determining the heat transferred in the test section $\dot{Q}_{TS}$ and it is connected to the cryocooler. The cryocooler cools the whole cold part of the setup, i.e. everything inside the vacuum chamber. The part of the test tube located within the copper block has a length $L = 5$ cm and is from now on referred to as the test section.

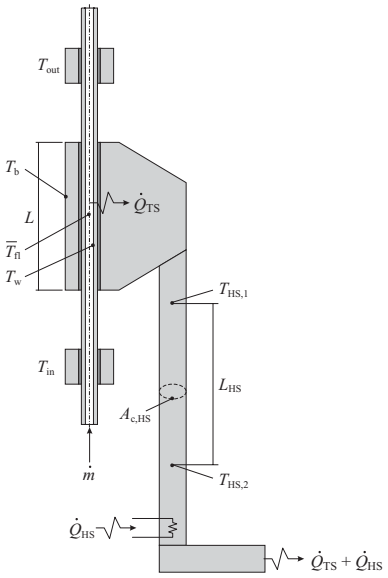

Figure 5: Details of the test section.

The temperature sensors T_{in} and T_{out} are inserted into two small copper blocks which are soft soldered on each side of the test section. The sensor T_b is inserted into the copper block close to the test tube, while $T_{HS,1}$ and $T_{HS,2}$ are inserted into the copper rod and measure $\dot{Q}_{TS}$.

The vacuum chamber is a stainless steel tank and measurements are carried out at a pressure of approx. 10^{-5}

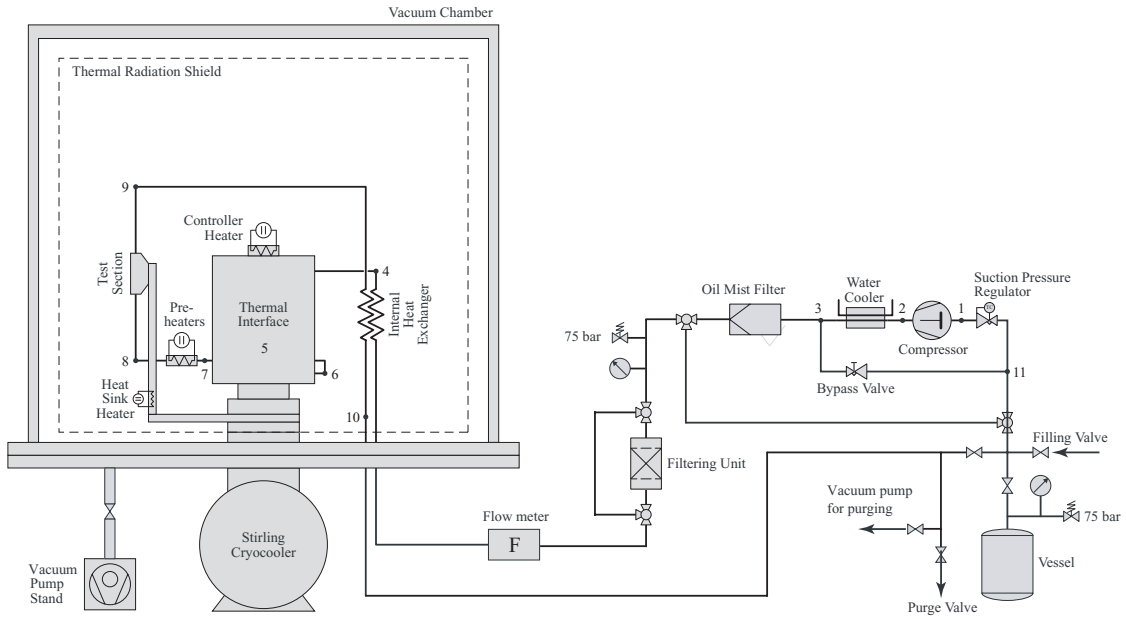

Figure 3: Schematic overview of the heat transfer test rig.

mbar. A thin copper plate is thermally connected to the cryocooler and placed around the above mentioned components to shield them from the radiation from the inside of the vacuum chamber, which is at ambient temperature.

Measurement Concept

The measured heat transfer coefficient $\overline{U}$ is a relation between the heat flux and the mean temperature difference between the fluid flow and the tube wall and is expressed by

$$\overline{U} = \frac{\dot{Q}_{TS}}{A_w \cdot \Delta T_{m,b}}, \tag{19}$$

where $\overline{U}$ is the mean heat transfer coefficient over the tube length, $\dot{Q}_{TS}$ is the heat load from the test section, A_w is the area of the wetted surface inside the tube, and $\Delta T_{m,b}$ is the mean temperature difference. $\Delta T_{m,b}$ is given by the logarithmic mean temperature difference,

$$\Delta T_{m,b} = \frac{T_{in} - T_{out}}{\ln\left(\frac{T_{in}-T_b}{T_{out}-T_b}\right)}, \tag{20}$$

for single phase flow, and

$$\Delta T_{m,b} = \frac{T_{in} + T_{out}}{2} - T_b, \tag{21}$$

for two phase flow. This supposes that the specific heat value c_p is constant through the test section, something that can be assumed for small temperature differences between the inlet T_{in} and outlet T_{out} bulk temperatures. T_b is the temperature close to the tube wall. Equations (20) and (21) are also only valid as long as the wall temperature is constant in the flow-direction along the flow channel, something that can be assumed in this case due to the use of high conductive copper.

As the actual wall temperature T_w is not equal to the measured temperature T_b, $\overline{U}$ is modified to obtain the heat transfer coefficient $\overline{h}$ at the tube wall. This is done by modelling a thermal resistance R_{eff} between the location of the sensor T_b and the tube wall.

$$\overline{U} = \frac{1}{(R_h + R_{\text{eff}}) \cdot A_w} = \frac{1}{\left(\frac{1}{\overline{h}} + R_{\text{eff}}\right) \cdot A_w}, \tag{22}$$

$$\overline{h} = \frac{\overline{U}}{1 - \left(\overline{U} \cdot A_w \cdot R_{\text{eff}}\right)}, \tag{23}$$

where R_h expresses the resistance by convection at the wetted surface. R_{eff} is here a thermal resistance between the tube wall and the location of T_b, which comprises of layers of copper, tin solder and the steel tube. A series of turbulent liquid flow measurements at different Reynolds

numbers are used to find R_{eff} by regression analysis, assuming that Equation (18) also applies for tubes with diameter around 1 mm. This is referred to as a Wilson plot method described by e.g. Pettersen [24]. Regression software is used to find R_{eff} directly from the measured data. To develop a useful fit function for this, Equation (23) is rewritten to

$$\frac{1}{\overline{U}} = \frac{1}{\overline{h}} + R_{\text{eff}} \cdot A_w = \frac{d_h}{Nu \cdot k} + R_{\text{eff}} \cdot A_w, \qquad (24)$$

and inserting Equation (18) for the Nusselt-number yields

$$\frac{1}{\overline{U}} = \frac{d_h/k}{0.012\,(Re^m - 280)\,Pr^{0.4}\left[1 + \left(\frac{d}{L}\right)^{\frac{2}{3}}\right]\left(\frac{\mu}{\mu_w}\right)^{0.25}} + R_{\text{eff}} \cdot A_w, \qquad (25)$$

where k is the conductivity of the fluid.

The test facility is mainly designed to do tests on condensing fluids, therefore the heat transferred from the fluid $\dot{Q}_{TS}$ not measured by a heat balance on the fluid. Referring to Figure 5, $\dot{Q}_{TS}$ is calculated by measuring the temperature difference between $T_{HS,1}$ and $T_{HS,2}$, and by knowing the length L_{HS}, the area $A_{C,HS}$ and the thermal conductivity k_{Cu} of the copper.

$$\dot{Q}_{TS} = \frac{k_{Cu}}{L_{HS}} \cdot A_{C,HS} \cdot \left(T_{HS,1} - T_{HS,2}\right) \cdot C_1 + C_2. \qquad (26)$$

The coefficients C_1 and C_2 are calibrated using a heat balance for liquid flow through the test section as a reference.

Tube diameter

Grohmann [19] stressed that the roughness in small tubes makes the wetted surface A_w noticeably larger than in a smooth tube with the same diameter. Therefore, two diameters were defined; d_w estimated from the actual perimeter P of the tube,

$$d_w = \frac{P}{\pi}, \qquad (27)$$

and d_c from the measured cross-sectional area A_c of the tube,

$$d_c = \sqrt{\frac{4A_c}{\pi}}. \qquad (28)$$

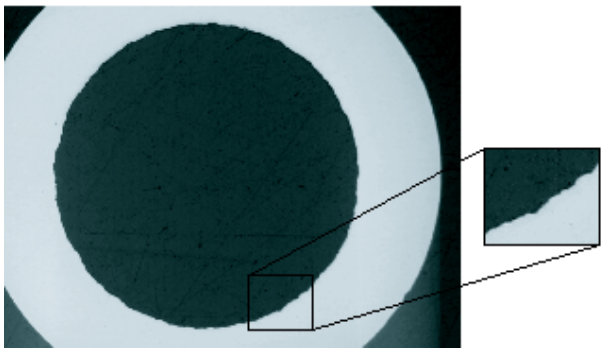

Figure 6: Microscope photo of the test tube used for determining d_w and d_c in the heat transfer test rig.

The diameter d_w is relevant for heat transfer related quantities such as the Nusselt number, while d_c is relevant for mass flow related quantities such as the Reynolds number. Both of them were found using photos of the tube at six different locations, one of these photos is shown in Figure 6 and a morphology software calculated the perimeter and cross-sectional area.

Measurement program

After a period of careful verification and calibration, the experimental program will start by finding R_{eff} for the tube first installed ($d = 1$ mm). After this, experiments with both liquid and vapour methane will be done. Experiments with condensing methane will then be carried out, at different heat flux, flow rate and vapour quality. After this, tests with natural gas like mixtures, with e.g. 90 % methane and 10 % ethane will take place. Mixtures with a non-condensable component, e.g. nitrogen can also be done.

Further, the test tube will be replaced by tubes of different diameter, e.g. 500 μm and 250 μm or 2 mm, in order to investigate the diameter dependence on heat transfer and pressure drop. R_{eff} will have to be found for each new tube and other relevant parts of the measurement program will be repeated.

EXPERIMENTS ON MICRO-SCALE FLOW PHENOMENA

This experimental effort aims at improving the understanding of micro-scale two-phase flow phenomena as

droplet-droplet interaction and liquid film flow behavior. An experimental setup with a high-speed camera and laser for visualisation is proposed. It is expected that one will be able to acquire data of two-phase flow phenomena at the micro-scale level under various conditions. The experiments will be done with different geometries, droplet velocities and liquid film thickness.

Research methodology

Detailed experiments on mixed refrigerants at low temperatures are cumbersome to perform. It has therefore been decided to do experiments with a test fluid consisting of 80% pentane and 20% iso-octane. The test fluid represents fairly comparable physical properties at a more operable condition (60°C and 1.1 bar) compared to mixed refrigerants in the heat exchanger [25].

As the experimental research focus will be on the physical interaction mechanisms of micro-scale flow phenomena, laser-based visualization techniques [26] will be used. The experimental setup integrates three parts: the first part is a test section where the phenomena are located; the second part is the light source part in which a backlight or a laser will be utilized for the illumination of the phenomena; the third part is the picture capturing part in which a camera, either a high speed or fast gated camera, will be employed to record the phenomena, giving results in terms of time- and spatial-resolved pictures. For the study of the fast-evolving flow interaction processes, a Phantom series version 9.1 high speed camera will be used [27].

The test section will be a gas-tight box flushed with test fluid gas. It will be maintained at the relevant temperature and pressure with transparent walls for laser and camera light access. Within the test section, regarding the geometries where the concerned phenomena take place, it is decided to start with a horizontal plate with stagnation liquid film of different thickness. The plate may be designed rotating, and thus later it can be inclined for the study of flowing liquid film on the plate. Afterwards, the plate may be replaced by a tubular geometry which gives a more relevant geometry considering the tubular geometry inside the spiral wound heat exchanger. A specially designed slit will be used for liquid film generation.

A simple sketch of the experimental setup is shown in Figure 7.

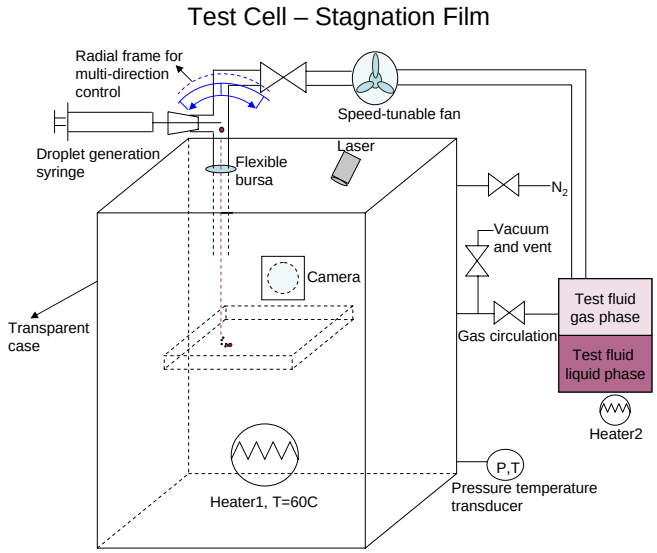

Figure 7: Simple sketch of the experimental setup study stagnation liquid film.

As the experimental research progresses, the experimental setup will be changed to different arrangements in which the focused geometries are simply drawn in Figure 8, where the liquid films on the geometries are marked by using plum color.

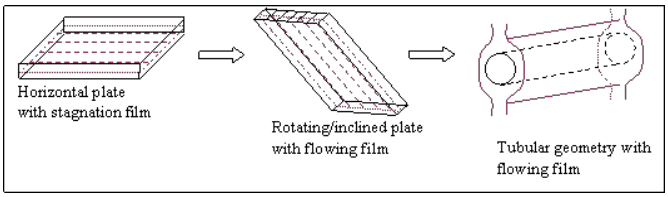

Figure 8: Research focused geometry evolution.

It is expected that the experimental results will explore the relations between the different phenomena discussed earlier in the article. These relations are of great importance to the development of numerical simulation of components in a heat exchanger, and the experimental results will also be used to verify the numerical computations. Specific issues to be examined are listed below.

In terms of droplet-gas interaction:

- Description of trajectory and deformation of different size droplets.
- Experimentally and numerically investigation of ve-

locities of different size droplets.

In terms of droplet interaction with solid and liquid surface:

- Description of the interaction process.
- Contact angle (interaction with solid surface).
- Splashing threshold (interaction both with solid surface and liquid surface).
- Coalescence threshold (interaction with liquid surface).
- Qualified and quantified description of other phenomena such as gas entrapment and satellite droplet formation.

In terms of droplet-droplet interaction:

- Description of the interaction process.
- Coalescence threshold.
- Qualitative and quantitative description of satellite droplet formation.

CONCLUSIONS

To develop compact heat exchangers that reduce cost and production time compared to the spiral wound heat exchanger, more knowledge of microscale two-phase flow is needed. To provide this knowledge, a combined research strategy of experiments and computations on basic phenomena is presented. A possible experimental setup has been outlined, aimed towards providing detailed experimental data of small-scale phenomena. Besides providing more knowledge in it self, the data will be valuable for the development of the computational method. For us to be able to compute integral quantities as pressure drop and heat transfer of new designs, the computational method must capture the underlying phenomena. Then to provide data for the design of compact heat exchangers and to give a well-defined verification data for the numerical method, an experimental setup has been built for measuring integral quantities such as heat transfer and pressure drop of fluids in small tubes at low temperatures.

ACKNOWLEDGMENT

This publication forms a part of the Remote Gas project, performed under the strategic Norwegian Research program Petromaks. The authors acknowledge the partners; Statoil, Hydro, UOP, Aker Kværner, DNV, and the Research Council of Norway (168223/S30) for support.

REFERENCES

[1] S. Mokhatab. Breaking the offshore LNG stalemate. *World Oil*, 228(4), 2007.

[2] Ralph L. Webb and Nae-Hyun Kim. *Principles of Enhanced Heat Transfer*. Taylor & Francis Group, 270 Madison Avenue, New York, 2nd edition, 2005.

[3] J. F. Roques and J. R. Thome. Falling film transitions between droplet, column and sheet flow modes on a vertical array of horizontal 19 fpi and 40 fpi low-finned tubes. *Heat Transfer Engineering*, 24(6):40–45, 2003.

[4] Z. Mohanmed-Kassim and E. K. Longmire. Drop impact on a liquid-liquid surface. *Physics of Fluids*, 15:3263–3273, 2003.

[5] G. A. Bach, D.L. Koch, and A. Gopinath. Coalescence and bouncing of small aerosol droplets. *Journal of Fluid Mechanics*, 518:157–185, 2004.

[6] M. Rein. Phenomena of liquid drop impact on solid and liquid surfaces. *Fluid Dynamics Research*, 12: 61–93, 1993.

[7] A. B. Wang and C. C. Chen. Splashing of a single drop onto very thin liquid films. *Physics of Fluids*, 12:2155–2158, 2000.

[8] C. D. Stow and M. G. Hadfield. An experimental investigation of fluid flow resulting from the impact of a water drop with and unyielding dry surface. *In Proceedings of the Royal Society of London, Series A*, 373:419–441, 1981.

[9] P.A. Kew and K. Cornwell. Correlations for the prediction of boiling heat transfer in small-diameter channels. *Applied Thermal Engineering*, 17:705–715, 1997.

[10] John R. Thome. Fundamentals of boiling and two-phase flows in microchannels. 2006. Keynote lecture at 13th International Heat Transfer Conference, Sydney, Australia.

[11] R.W. Lockhart and R.C. Martinelli. Proposed correlation of data for isothermal two-phase two-component flow in a pipe. *Chem. Eng. Prog.*, 45, 1949.

[12] D. Chisholm. Pressure gradients due to friction during the flow of evaporating two-phase mixtures in smooth tubes and channels. *Int J Heat Mass Transfer*, 16, 1973.

[13] L. Friedel. Improved friction pressure drop correlations for horizontal and vertical two-phase pipe flow. *European Two-Phase Flow Group Meeting*, 1979.

[14] D. Chisholm. *Two-phase flow in pipelines and heat exchangers*. George Godwin, 1983.

[15] H. Müller-Steinhagen and K. Heck. A simple friction pressure drop correlation for two-phase flow in pipes. *Chem. Eng. Process.*, 20:297–308, 1986.

[16] D. A. Drew and S. L. Passman. *Theory of Multicomponent Fluids*. Number 135 in Applied Mathematical Sciences. Springer-Verlag, New York, 1999. ISBN 0-387-98380-5.

[17] K.E. Teigen and R. Olsen. Examining the level-set methods applicability for computations of transient two-phase flow of natural gas. In *5th International Conference on Heat Transfer, Fluid Mechanics and Thermodynamics*, 2007.

[18] Mark Sussman, Peter Smereka, and Stanley Osher. A level set approach for computing solutions to incompressible two-phase flow. *J. Comput. Phys.*, 114:146–159, 1994.

[19] S. Grohmann. Measurement and modeling of single-phase and flow-boiling heat transfer in microtubes. *International Journal of Heat and Mass Transfer*, 48:4073–4089, 2005.

[20] V. Gnielinski. New equations for heat and mass transfer in turbulent pipe and channel flow. *Int. Chem. Eng.*, 16:359–368, 1976.

[21] W. M. Kays, M. E. Crawford, and B. Weigand. *Convective Heat and Mass Transfer*. McGraw-Hill, New York, 4th edition, 2005.

[22] B.S. Petukhov. *Advances in Heat Transfer*, volume 6. Academic Press, 1970.

[23] S. Grohmann. Design and operation of the compact LNG heat exchanger test stand. Technical report, unpublished, SINTEF Energy Research, 2004.

[24] J. Pettersen. *Flow Vapourization of CO2 in Microchannel Tubes*. dr. techn. thesis, Norwegian University of Science and Technology (NTNU), 2002.

[25] T. Lex, K. Ohlig, A. O. Fredheim, and C. B. Jenssen. Ready for floating LNG - qualification of spiral wound heat exchangers. In *Proceedings 15th International Conferences on Liquefied Natural Gas*, 2007.

[26] A. Frohn and N. Roth. *Dynamics of droplets*. Springer, first edition, 2000.

[27] *Introduction to the product Phantom V9.1 of Vision Research Inc.* URL `www.visionresearch.com`.